Collision energy-resolved study of the emission cross-section and the Penning ionization cross-section in the reaction of BrCN with He *(2 3 S)

ARTICLE *in* CHEMICAL PHYSICS LETTERS · DECEMBER 2001

Impact Factor: 1.9 · DOI: 10.1016/S0009-2614(01)01223-4

3 AUTHORS, INCLUDING:

Yoshihiro Yamakita
The University of Electro-Communicat…

30 PUBLICATIONS **581** CITATIONS

SEE PROFILE

7 December 2001

ELSEVIER

Chemical Physics Letters 349 (2001) 411–420

CHEMICAL PHYSICS LETTERS

www.elsevier.com/locate/cplett

Collision energy-resolved study of the emission cross-section and the Penning ionization cross-section in the reaction of BrCN with $He^*(2^3S)$

Kazuhiro Kanda [a,*], Yoshihiro Yamakita [b,1], Koichi Ohno [b,1]

[a] *Laboratory of Advanced Science and Technology for Industry, Himeji Institute of Technology, 3-1-2 Kouto, Kamigori, Ako, Hyogo 678-1205, Japan*

[b] *Department of Chemistry, Graduate School of Science, Tohoku University, Aramaki, Aoba-ku, Sendai 980-8578, Japan*

Received 26 July 2001; in final form 20 September 2001

Abstract

The dissociative excitation of BrCN producing $CN(B^2\Sigma^+)$ fragment by the collision of $He^*(2^3S)$ was investigated by the collision energy-resolved electron and emission spectroscopy using time-of-flight method with a high-intensity He^* beam. The Penning electrons ejected from BrCN and the subsequent $CN(B^2\Sigma^+–X^2\Sigma^+)$ emission were measured as a function of collision energy in the range of 90–180 meV. The formation of $CN(B^2\Sigma^+)$ is concluded to proceed dominantly via the promotion of an electron from Π-character orbital, by comparison between the collision energy dependence of the partial Penning ionization cross-sections and the $CN(B^2\Sigma^+–X^2\Sigma^+)$ emission cross-section.

1. Introduction

An excited CN radical is produced efficiently in the dissociative excitation of cyanogen halide by a rare-gas atom in its metastable excited state. Many studies have been made on the dissociative excitation of BrCN from the observation of the subsequent $CN(B^2\Sigma^+–X^2\Sigma^+)$ [1–7] and $CN(A^2\Pi_i–X^2\Sigma^+)$ emission [8], but the reaction process and the precursor state producing the excited CN fragment have not been fully understood. The pioneering work of the dissociative excitation of BrCN with $He^*(2^3S)$ was reported by Fukuda [9] and relatively intense CN(B–X) emission was observed from BrCN in a He flowing afterglow,

$$He^*(2^3S) + BrCN \rightarrow CN(B–X). \quad (1)$$

In the collisional reaction of helium metastable atom $He^*(2^3S)$ with BrCN, we can observe not only the subsequent emission from excited CN fragments but the free electrons by Penning ionization, because the excitation energy of $He^*(2^3S)$ 19.82 eV is higher than the ionization potential of BrCN, 11.88 eV [10],

* Corresponding author. Fax: +81-792-58-0476.

E-mail addresses: kanda@lasti.himeji-tech.ac.jp (K. Kanda), yy@qpcrkk.chem.tohoku.ac.jp (Y. Yamakita), ohnok@qpcrkk.chem.tohoku.ac.jp (K. Ohno).

[1] Fax: +81-22-217-6580.

0009-2614/01/$ - see front matter
PII: S0009-2614(01)01223-4

$$He^*(2^3S) + BrCN \rightarrow He + BrCN + e^-. \quad (2)$$

Penning ionization electron spectrum (PIES) of BrCN has been investigated in the range of 0–10 eV by Yee and Brion [11].

In Penning ionization, when a metastable atom approaches a target molecule, an electron can transfer from the outer orbital of a target molecule to the vacant inner-shell orbital of a metastable atom and an electron is ejected from the outer orbital of a metastable atom simultaneously. Penning ionization cross-section is governed by exterior part of electron density of molecular orbital to be ionized, since the collisional process occurs around outer part of the target molecule [12,13]. Collision energy dependence of the total ionization cross-section in Penning ionization reflects the interaction potential between He^* and a target molecule. For an isotropic target system, a simple model for collision energy dependence of the partial ionization cross-section (CEDPICS) has been established [14,15]. This is the simplest model which could be applicable to anisotropic molecules in an analogy manner. The CEDPICS of various molecules have been studied with this model, together with the molecular-orbital (MO) calculations of the interaction potential between He^* and the molecule [16–21].

The subsequent emission from excited products represents the distribution of final products in the reaction, whereas Penning ionization electron reflects the molecular orbitals excited initially when the metastable atom approaches the target molecule. The emission cross-section reflects the cross-section for the production of the relevant states connecting with the final products, and the branching ratio from those states to final products. Therefore, the measurements of Penning electron and fragment emission give us the information on the properties of entrance channel and exit channel, respectively, in the collisional reaction of the metastable atom with the target molecule. By comparison of collisional energy dependence of the emission cross-section with those of the partial ionization cross-sections, the important knowledge of reaction dynamics can be obtained, such as the correlation of initially excited molecular orbitals and final state distributions.

In the present study, we have developed the experimental method by addition of an optical detection system to the CEDPICS apparatus. The subsequent CN(B–X) emission produced in the collisional reaction of $He^*(2^3S)$ with BrCN was measured as a function of collision energy in the range of 90–180 meV, as well as the Penning electron from BrCN. We discussed the anisotropic characteristics of the interaction potential between He^* and BrCN by comparison of CEDPICS with the molecular orbital (MO) calculations and investigated the reaction mechanism of the dissociative excitation producing CN(B) in the collision of $He^*(2^3S)$ with BrCN on the basis of the collision energy dependence of the emission cross-section.

2. Experimental

The experiments were carried out using the high-intensity He^* beam apparatus reported previously [16,17], after the modification for optical measurements [22]. Metastable atoms of He^* were produced by a discharge nozzle source with a tantalum hollow cathode [17] and $He^*(2^1S)$ component was quenched by a water-cooled He dc lamp. The $He^*(2^3S)$ beam flux was about 1×10^{15} atoms s^{-1} sr^{-1}. The metastable $He^*(2^3S)$ beam was chopped with a mechanical chopper of pseudo-random type rotating at 300 Hz and introduced into a collision cell. The kinetic energy E_e of an ejected electron was measured by use of a hemispherical electrostatic deflection-type analyzer perpendicularly to the incident $He^*(2^3S)$ beam. The resolution of the electron energy analyzer was 250 meV for collision energy-resolved measurements. Time-of-flight (TOF) signal of $He^*(2^3S)$ was obtained by detecting secondary electrons emitted from a stainless steel plate covered with sample gas in the collision cell. Collision energy-resolved spectra were obtained by a time-correlation TOF method and a two-dimensional data accumulation system [20].

The details about an optical detection system are described in the forthcoming paper [22]. Briefly, fluorescence was collected in a direction orthogonal to the He beam through a quartz

window attached on a side wall of the collision cell and focused by a quartz lens ($f = 21$ cm) onto the entrance slit of a 25-cm monochromator (Nikon G250) equipped with a grating blazed at 500 nm. The dispersed emission was detected by a bi-alkali photomultiplier tube (Hamamatsu R585). A typical spectral resolution was 3.1 and 5.8 nm (FWHM) for the measurement of CN(B–X) emission spectrum and the collision energy dependence of the emission cross-section, respectively. The spectral response of the monochromator and the detection system was calibrated by using a standard halogen lamp (Phoenix). BrCN (Nakarai, ~90%) was introduced into the collision cell after a trap-to-trap cycle in order to eliminate possible impurities, especially H_2O.

3. Results and discussions

3.1. CN(B–X) emission spectrum

Fig. 1 shows the CN(B–X) emission spectrum produced in the collisional reaction of BrCN with $He^*(2^3S)$. The transition frequencies of the CN(B–X) emission and the molecular constants of CN(B) radical [23] have been reported previously in detail. In the present study, three sequences of CN(B–X) emission ($\Delta v = 0$ and ± 1) were observed in the 330–440 nm region. The observation of the 1–0 sequence indicates the production of CN(B) in the $v' = 1$ state. By taking the Franck–Condon factors into account, the ratio of vibrational populations is estimated to be $P_{v'=1}/P_{v'=0} < 0.2$. The 0–0 sequence is observed to be degraded to violet, which corresponds to that the 0–0 band head of the CN(B–X) emission arises in the P branch (at $N = 28$). No emission of other species, for example Br atom, was observed in the wavelength range 300–500 nm. The CN(B–X) emission spectrum in the collisional reaction of BrCN with $He^*(2^3S)$ was measured by using flowing afterglow method with a high resolution (0.04 nm FWHM) [9]; the vibrational bands of $v' = 0$, 1 and 2 were observed, and the vibrational band of $v' = 0$ was dominant among them. This result at the thermal collision energy region is consistent with the observed spectrum in the collision energy range of 90–180 meV in the present study.

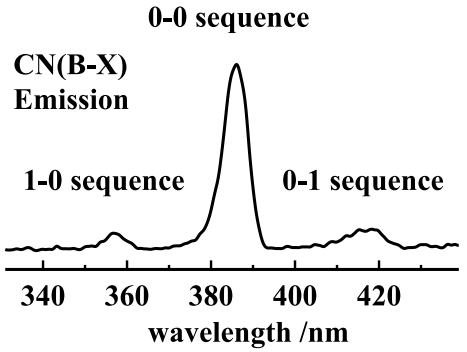

Fig. 1. Observed emission spectrum of the CN($B^2\Sigma^+$–$X^2\Sigma^+$) transition in the $He^*(2^3S)$ + BrCN reaction.

The absolute cross-section for the CN($B^2\Sigma^+$–$X^2\Sigma^+$) emission in the $He^*(2^3S)$+ BrCN reaction was roughly estimated by the comparison with the known emission cross-section for the reaction,

$$He^*(2^3S) + N_2 \rightarrow He + N_2^+(B^2\Sigma^+) + e^-. \quad (3)$$

The absolute emission cross-section of $N_2^+(B^2\Sigma^+–X^2\Sigma^+)$ in process (3) was reported to be $\sim 3 \times 10^{-20}$ m^2 in the collision energy range of 0.03–0.16 eV [24]. The transition frequency $hc\nu_{00}(CN(B–X)) = 3.19$ eV and the radiative lifetimes of CN(B) $\tau(CN(B)) = 62$ ns are very close to the transition frequency $hc\nu_{00}(N_2^+(B–X)) =$ 3.17 eV and the radiative lifetimes of $N_2^+(B^2\Sigma^+)$ ions $\tau(N_2^+(B)) = 63$ ns [23]. The integrated intensity of the CN(B–X) emission was compared with that of the N_2^+(B–X) emission observed at the same sample pressure. The details of scaling procedure were described in [25]. The emission cross-section of CN(B–X) σ_{em} was estimated to be $\leqslant 1 \times 10^{-20}$ m^2. The obtained emission cross-section corresponds to the cross-section for the production of CN(B), because the radiative decay was the dominant process for the CN formed in the B-state.

3.2. Penning ionization electron spectrum

The valence electron configuration of BrCN in the ground state can be written as

$$(1\sigma)^2(2\sigma)^2(3\sigma)^2(1\pi)^4(4\sigma)^2(2\pi)^4;\ {}^1\Sigma^+. \quad (4)$$

The nature of each MO has been studied in detail by photoelectron spectroscopy [10,26,27]. The 1π and 2π MOs originate from the combination of the 4p orbital of Br atom and the π bonding orbital of CN group in phase and out of phase, respectively. The 4σ orbital can be regarded primarily as the lone-pair localized on N atom. Fig. 2 shows the $He^*(2^3S)$ Penning ionization electron spectrum of BrCN. Three ionic states were observed in the electron energy range of 3–9 eV, which correspond to the electrons ejected from the 2π, 4σ and 1π MOs, respectively. The first band, arising from ejection of the degenerated 2π orbitals, has similar band intensity at both spin sub-level in the photoelectron spectrum [10,26,27], however the intensity at $^2\Pi_{3/2}$ level is much smaller than that of $^2\Pi_{1/2}$ level in the PIES. The band intensity of the 4σ band is much larger than that of the 2π band in the PIES, whereas the similar intensities of both bands were observed in the photoelectron spectrum [10,26,27]. Peak energy shift in PIES measured with respect to the nominal energy E_0 (E_0 is the difference between the metastable excitation energy and the target ionization potential) reflects the interaction potential between target molecule and $He^*(2^3S)$ [28]. From the large negative peak energy shift, 260 meV, observed at the 4σ band, an attractive potential surface is expected. Lower electron energy regions of 0–3 eV for PIES could not be observed in the present experiment, because of the low transmission of the electron spectrometer in that energy region. The PIES of BrCN was reported previously by Yee and Brion [11]. Observed spectral features and peak energy shifts are in good agreement with their work.

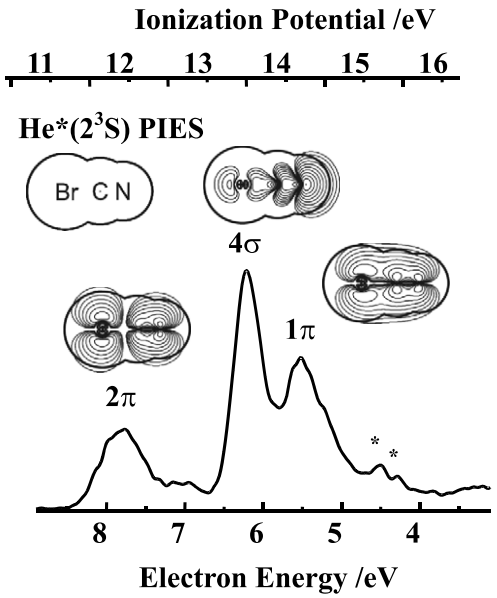

Fig. 2. $He^*(2^3S)$ Penning ionization electron spectrum of BrCN. Asterisks denote impurity N_2 bands.

Molecular orbital (MO) calculations were performed with a quantum chemistry program package [29], for the purpose of discussion on the nature of MOs of BrCN. The nuclear distances of Br–C and C–N were initially derived from the literature [26] and optimized by the MO calculation. The 6-311++G** basis set was used for C and N atoms, and the aug-cc-pVTZ basis set was used for Br atom. In spin-unrestricted DFT calculations, the B3LYP function was used for exchange-correlation potential. The electron density maps obtained from the MO calculations were drawn for the relevant molecular orbitals in Fig. 2. Thick lines in the electron density maps represent the repulsive molecular surfaces estimated from the van der Waals radii of atoms ($r_C = 1.7$ Å, $r_N = 1.5$ Å, $r_{Br} = 1.95$ Å). The 2π and 1π MOs exposed outside the molecular surface of BrCN in the orthogonal direction to the molecular axis around CN bond. While, the 4σ orbital exposed outside the molecular surface along the molecular axis around N atom.

One of the most significant aspects of PIES is that an outer orbital gives a strong band and the inner orbital yields a weak band [12,13]. The large cross-section for the 4σ orbital in PIES is clearly interpreted with the electron distribution of this orbital, which is extending outside of the N atom and easily attacked by metastable helium atoms. The enhancement of band intensity, which corresponds to the electron ejected from the 'lone pair' σ orbital localized on the N atom of the CN group, has been also reported in the PIES of some nitriles and thiocyanic methyl [18–20,30,31]. This strong enhancement was ascribable to be the

behavior of the 'lone pair' σ electrons as an sp hybrid orbital extending outside on the CN axis.

3.3. Interaction potential between BrCN and $He^*(2^3S)$

In Penning ionization process, the collision energy E_c dependence of the total ionization cross-section reflects the interaction potential between a metastable atom and a target molecule. For an isotropic target system, a simple model for collision energy dependence of the partial ionization cross-section, $\sigma_i(E_c)$, has been established by Illenberger and Niehaus [14,15]. In general, negative inclination of the $\log\sigma_i(E_c)$ vs $\log E_c$ plots indicates the attractive interaction between a metastable atom and a target molecule, and positive inclination reflects the repulsive interaction. This model is approximately applicable to an anisotropic target molecule. Since the exterior electron density of a molecular orbital is generally localized at some parts of the molecular surface (Fig. 2) and Penning ionization occurs at the parts where electron density extends, CEDPICS gives us an information on the anisotropic interaction potential between a metastable atom and a target molecule.

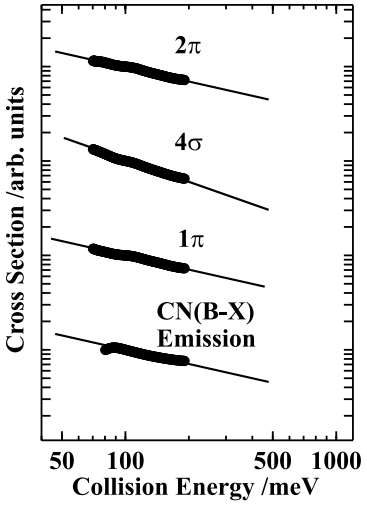

Fig. 3. Collision energy dependence of partial ionization cross-sections for BrCN with $He^*(2^3S)$ and the CN(B–X) emission cross section in the collisional reaction of $He^*(2^3S)$ with BrCN.

Fig. 3 represents the $\log\sigma_i$ vs $\log E_c$ plots of CEDPICS for the 2π, 4σ and 1π MOs of BrCN in the collision energy range of 90–180 meV. The $\log\sigma_i$ decreases with increasing $\log E_c$ for these three bands as shown in Fig. 3, which indicates that an attractive interaction exists between BrCN and He^*. When the potential curve for the entrance channel is approximated by a long-range attractive potential $V^*(r)$ as follows:

$$V^*(r) \propto r^{-s}, \tag{5}$$

the cross-section σ_i can be expressed by [14,15,32]

$$\sigma_i \propto E_c^{-2/s}. \tag{6}$$

The values of s obtained from a least-square fitting of slope m of the $\log\sigma_i$ vs $\log E_c$ plots are listed in Table 1. The value of s for the 4σ band, 2.7 ± 0.2, is smaller than those for the 2π band, 4.1 ± 0.4, and the 1π band, 4.3 ± 0.4. When He^* approaches the N end of BrCN along the CN axis, the attractive interaction is stronger than that in the case of the approach in the perpendicular direction to the molecular axis.

The calculation of interaction potentials between BrCN and metastable helium atom were carried out by using the quantum chemistry package [36] in order to discuss the collision of BrCN with $He^*(2^3S)$. A $Li(2^2S)$ atom was used in

Table 1
Ionization potentials of BrCN and observed slope parameters

Ionic state	Orbital	Character	IP_{obsd}[a] (eV)	m	s
$X^2\Pi$	2π	π_{CN}	11.88, 12.07	-0.49 ± 0.04	4.1 ± 0.4
$A^2\Sigma^+$	4σ	σ_N	13.58	-0.73 ± 0.04	2.7 ± 0.2
$B^2\Pi$	1π	π_{CN}	14.4	-0.46 ± 0.04	4.3 ± 0.4
$CN(B^2\Sigma^+–X^2\Sigma^+)$ emission				-0.47 ± 0.05	4.3 ± 0.4

[a] Ref. [10].

place of $He^*(2^3S)$, because the resemblance between $He^*(2^3S)$ and $Li(2^2S)$ is well known (see [14,16] and references cited therein). The 6-311++G** basis set was used for Li atom. Calculated Li–BrCN interaction potential curves from the interaction potentials $V^*(r)$ with BrCN and a metastable helium atom along different directions are shown in Fig. 4. In the case of the access of the Li atom to the N atom along the molecular axis (case A), the potential is smoothly decreased and an attractive well of ~500 meV depth exists at the Li–N nuclear distance around 1.9 Å. For the access to the Br atom (case B), the repulsive potential wall exists at the Li-Br nuclear distance of ~2.5 Å. For access to BrCN from perpendicular direction to the molecular axis (case C), a small attractive well exists at the distance between Li and molecular axis of ~2.3 Å. A deep attractive potential around N end can account for the large negative inclination of CEDPICS of the 4σ band. The large negative peak shift (≈ −260 meV) supports this conclusion. On the contrary, a small attractive well

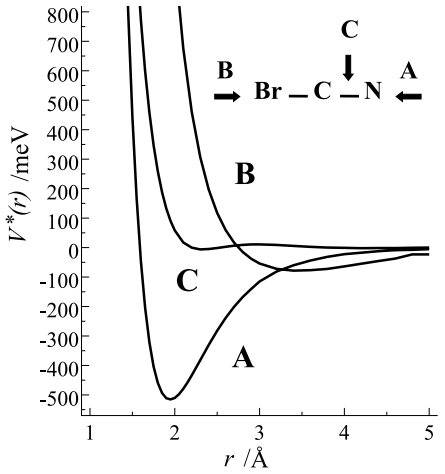

Fig. 4. Calculated interaction potential curves between BrCN and Li: (A) the potential curve for the access to the N atom along the molecular axis, r represents the nuclear distance between the N atom and the Li atom; (B) the potential curve for the access to the Br atom along the molecular axis, r represents the nuclear distance between the Br atom and the Li atom; (C) the potential curve for the access to the center of the CN bond in the direction of perpendicular to the molecular axis, r is the distance between the molecular axis and the Li atom.

in the perpendicular direction to the molecular axis is compatible with the relatively small negative inclination of CEDPICS of the 2π and 1π bands. The large negative inclination of the σ_N band and the small negative inclination of π_{CN} band in the $\log\sigma_i$ vs $\log E_c$ plots of CEDPICS were also reported in the CEDPICS investigation of acetonitrile [19].

3.4. Reaction mechanism of dissociative excitation producing the CN(B) fragments

The major process of the reaction of BrCN with He^* is the non-radiative Penning ionization. The emission cross-section of CN(B–X) was estimated to be $\leqslant 1\times10^{-20}$ m^2, as described in Section 3.1. This small cross-section suggests that the direct collision mechanism is rather preferable than the collision complex formation, on the CN(B) formation. On the other hand, the CN(B) was concluded to be formed via the direct collision mechanism in dissociative excitation of BrCN with heavy rare-gas metastable atom, Rg^m (Rg = Ar, Kr, Xe) [3–8]. Therefore, it is unlikely that CN(B) is formed via the complex formation in the reaction of BrCN with He^*, because of its large excitation energy. On the assumption of the direct collision mechanism, three dissociation pathways are energetically possible:

(I) Neutral dissociative excitation, where an excited state of BrCN is an intermediate:

$$\begin{aligned} He^*(2^3S) + BrCN &\rightarrow He + BrCN^{**} \\ &\rightarrow He + Br \\ &\quad + CN(B^2\Sigma^+) \end{aligned} \tag{7}$$

(II) Ionization excitation – dissociative ionization, where a $BrCN^+$ ion is an intermediate:

$$\begin{aligned} He^*(2^3S) + BrCN &\rightarrow He + BrCN^+ + e^- \\ &\rightarrow He + Br^+ \\ &\quad + CN(B^2\Sigma^+) + e^- \end{aligned} \tag{8}$$

(III) Neutral excitation – dissociative ionization, where a neutral excited state of BrCN is an intermediate the same as mechanism I, but Br^+ ion is formed as a final product:

Table 2
Energetics of $He^*(2^3S)$ + BrCN reactions

Active species	Excitation energy (eV)
$He^*(2^3S)$	19.82
Product channel	**Energy of formation (eV)**
CN(X) + Br	3.60
CN(B) + Br	6.79
CN(G) + Br	11.12
CN(H) + Br	11.16
$CN(B) + Br^+$	18.60
$BrCN^+(X)$ $[2\pi^{-1}]$	11.88
$BrCN^+(A)$ $[4\sigma^{-1}]$	13.58
$BrCN^+(B)$ $[1\pi^{-1}]$	14.40

$$\begin{aligned} He^*(2^3S) + BrCN &\rightarrow He + BrCN^{**} \\ &\rightarrow He + Br^+ \\ &\quad + CN(B^2\Sigma^+) + e^- \end{aligned} \tag{9}$$

The main product channels of the collisional reaction of $He^*(2^3S)$ with BrCN and each formation energies are summarized in Table 2. Since $He^*(2^1S)$ component was quenched by a water-cooled helium discharge lamp, the excitation energy of the helium metastable atom is assumed to be the excitation energy of $He^*(2^3S)$ 19.82 eV. Ionization energy of Br atom IP(Br) = 11.81 eV and bond dissociation energy D_0(Br–CN) = 3.60 eV are used for the calculation of formation energies. The excitation energies of CN radicals are derived from the literature [23]. Exciplex formation, where an excited rare-gas cyanide, (Rg^+CN^-), is an intermediate, was so far proposed in the reaction of halogen cyanides with Xe^* [2,5]. However, this reaction pathway is not necessary to be considered in the reaction of BrCN with $He^*(2^3S)$, because it was excluded in the formation of CN(B) from the collision of BrCN with Ar^* [6].

The measurement of the collision energy dependence of the CN(B–X) emission cross-section (CEDECS) gives us the information on the property of molecular surface, where the molecular orbital relevant to the production of CN(B) extends towards outside. The dissociative excitation producing CN(B) proceeds initially by the excitation of an electron from a molecular orbital of BrCN with an approaching helium metastable atom. Therefore, by comparing CEDECS with CEDPICS, we can deduce the molecular orbital of BrCN which is relevant to the production of CN(B). The cross-section for the CN(B–X) emission σ_{em} is expressed by the product of the cross-section for excitation of an electron from relevant MO σ_{ex} and the branching fraction for the production of CN(B) relative to the total quenching when the orbital is excited. The reaction mechanism producing CN(B) is regarded as identical in the collision energy range of 90–180 meV, because the features in the CN(B–X) emission spectrum, for example the intensity ratio of the 1–0 sequence with the 0–0 sequence, observed at the collision energy of 90 meV resemble those observed at the collision energy of 180 meV, which indicates the rovibrational population of the produced CN(B) is not changed. Therefore, branching fraction Γ can be regarded as a constant in the present experimental energy range. When the long-range attractive part of the interaction potential plays a dominant role in the collisional reaction of $He^*(2^3S)$ with BrCN, σ_{em} is represented by

$$\sigma_{em} = \Gamma\sigma_{ex} \propto \Gamma E_c^{-2/s}. \tag{10}$$

Since the excitation energy of $He^*(2^3S)$ is much larger than ionization potential, the cross-section for the excitation of an electron from relevant MO σ_{ex} can be regarded almost the same as the cross-section for the ionization of an electron from corresponding MO. Therefore, the initially excited molecular orbital of BrCN, which leads to the dissociative excitation producing CN(B), can be discussed by the comparison of the s value for σ_{em} with σ_i.

The $\log\sigma_{em}(E_c)$ vs $\log E_c$ plot gives slope $m = -0.47 \pm 0.05$ (see Fig. 3). The s value, 4.3 ± 0.4, indicates that the molecular surface relevant to the production of CN(B) is fairly attractive. This value is not similar to that for the 4σ band, $s = 2.7 \pm 0.2$, but very close to those for the π bands, $s \approx 4.2$ in the range of 90–180 meV. It is concluded that the collisional dissociation producing CN(B) preferentially initiated by the promotion of a valence electron from 1π or 2π MO. This result conflicts simple parent/fragment state correlation. The main electronic configuration of the CN radical in the B state is

$$(1\sigma)^2(2\sigma)^2(3\sigma)^2(4\sigma)(1\pi)^4(5\sigma)^2;\ ^2\Sigma^+. \quad (11)$$

The MO correlation between a parent state, $BrCN^+$ cation (see Eq. (4)) and a fragment state, CN(B) predicted that the formation of CN(B) is related to the electron promotion from 4σ orbital of BrCN rather than the promotion of 1π or 2π electron. However, the ratio of quantum yields for production of the CN(A) and the CN(B) fragments are almost unity in the photoexcitation study of BrCN in the vacuum UV region using the synchrotron radiation [33,34]. Based on these results, the parent/fragment state correlation does not play an important role in the dissociative excitation of BrCN.

Reaction mechanism of dissociative excitation (1) is discussed on the basis of the above discussion and other experimental results. Mechanism I is a so-called 'energy transfer' reaction and favored in the formation of CN(B) from BrCN by the collision with a heavy rare-gas metastable [3,6,7]. However, it is unlikely that the Br atom is produced in the ground electronic state,

$$He^*(2^3S) + BrCN \rightarrow He + Br + CN(B^2\Sigma^+) \quad (12)$$

because an excess energy is too large in the present reaction, which is the excitation by the helium metastable. Therefore, the Br atom should be produced in some excited states. However, no neutral Br atom in the electronic excited state seems to be produced, because no atomic line of Br was observed. Otherwise, CN(B) is energetically producible via the following cascade processes:

$$He^*(2^3S) + BrCN \rightarrow He + Br + CN(H^2\Pi/G^2\Pi)$$
$$CN(H^2\Pi/G^2\Pi) \rightarrow CN(B^2\Sigma^+) + h\nu \quad (13)$$

However, the $CN(H^2\Pi) \rightarrow CN(B^2\Sigma^+)$ transition ($\nu_{00} = 35140.84\ cm^{-1}$) and the $CN(G^2\Pi) \rightarrow CN(B^2\Sigma^+)$ transition ($\nu_{00} = 34826.10\ cm^{-1}$) [23] have not observed in the present study. Therefore, it is concluded that the dominant dissociation pathway producing the CN(B) fragments is not a neutral dissociative excitation.

In mechanism II, a free electron is ejected from BrCN and CN(B) is produced from the dissociation of $BrCN^+$. If CN(B) was formed via this mechanism, the intermediate was ascribable to the $BrCN^+(X^2\Pi)$ or $BrCN^+(B^2\Pi)$ from the collision energy-resolved measurement as described in Section 3.2. In order to produce CN(B) via mechanism II, the excitation energy of the intermediate $BrCN^+$ is necessary to be larger than the sum of the bond dissociation energy $D_0(Br^+–CN)$ and excitation energy of CN(B). The minimum internal excess energies for producing CN(B) from the $BrCN^+(X^2\Pi)$ and $BrCN^+(B^2\Pi)$ are 6.72 and 4.20 eV, respectively. However, no vibrational progression, which can be ascribed to such excess energies, was observed in such an energy region of PIES (see Fig. 1). As a result, CN(B) is concluded to be produced via neutral excitation – dissociative ionization mechanism III.

The available excess energy E_{ex} for mechanism III amounts to 1.22 eV as listed in Table 2. Therefore, the ejected electron produced by mechanism III should be observed in the kinetic energy region $E_e < 1.22$ eV. The peak observed at ≈ 0.3 eV in the PIES [11] satisfies this requirement. This peak is assignable to the free electron produced by the autoionization of $Br(6p;\ ^2P^0, ^2D^0, ^2F^0)$ [35]. Accordingly, CN(B) and a free electron seem to be produced by the following dissociation process:

$$He^*(2^3S) + BrCN \rightarrow He + BrCN^{**}$$
$$BrCN^{**} \rightarrow Br(6p;\ ^2P^0, ^2D^0, ^2F^0) + CN(B^2\Sigma^+)$$
$$Br(6p;\ ^2P^0, ^2D^0, ^2F^0) \rightarrow Br^+ + e^- \quad (14)$$

In the vacuum UV photoabsorption spectrum of BrCN using the synchrotron radiation, numerous sharp peaks were observed in the wavenumber region below $1.1 \times 10^5\ cm^{-1}$, but no structural band was observed in the region $\approx 1.6 \times 10^5\ cm^{-1}$, corresponding to the excitation energy of $He^*(2^3S)$ [33,34]. It follows that the excitation by the collision of a rare gas metastable proceeds in a way completely different from that of optical excitation. For example, the collisional excitation with a rare gas metastable is able to produce optically forbidden states, such as a doubly excited state. As a result, CN(B) and the free electron observed at 0.3 eV in PIES are concluded to be formed from the dissociation of an optically forbidden superexcited state which is formed in the collisional reaction of $He^*(2^3S)$ with BrCN. The absence of corresponding peaks in the photoelectron spectra

[10,27] supports that the precursor state producing CN(B) is an optically forbidden state.

4. Conclusion

The collisional reaction of BrCN with $He^*(2^3S)$ producing CN(B) was investigated by the collision energy-resolved emission and electron spectroscopy by using the time-correlation TOF method with a high-intensity velocity-resolved $He^*(2^3S)$ beam. The partial Penning ionization cross-sections of orbitals and the CN(B–X) emission cross-section show negative collision energy dependence in the range of 90–180 meV. A deep attractive potential well was confirmed around the N end along the CN axis from the small *s* value for the 4σ band in this CEDPICS study and the result of quantum chemistry calculation. By the comparison of the collision energy dependence of the CN(B–X) emission cross-section with those of partial ionization cross-sections, the formation of CN(B) is concluded to proceed via the optically forbidden super-excited state by the promotion of an electron from a π-character orbital. The optical detection method used in the present work gives us direct information on the correlation between the initially excited orbitals and the final products, therefore it is applicable to variable reaction systems of the helium metastable atoms with molecules.

Acknowledgements

The authors are grateful to Professor K. Suzuki for his helpful discussion on the dissociative excitation of BrCN in a helium flowing afterglow. One of the authors (K.K.) wishes to thank Professor S. Katsumata for his continuous interest and Professor S. Matsui and Dr. Y. Haruyama for their encouragement. This research was partially supported by a Grant-in-Aid for Scientific Research from the Ministry of Education, Science, Sports and Culture.

References

[1] J.A. Coxon, D.W. Setser, W.H. Duewer, J. Chem. Phys. 58 (1973) 2244.
[2] R.J. Hennessy, Y. Ono, J.P. Simons, Chem. Phys. Lett. 75 (1980) 47.
[3] Y. Fukuda, K. Suzuki, T. Kondow, K. Kuchitsu, Chem. Phys. 87 (1984) 389.
[4] T. Nagata, T. Kondow, K. Kuchitsu, K. Tabayashi, S. Ohshima, K. Shobatake, J. Phys. Chem. 89 (1985) 2916.
[5] G.W. Tyndall, M.S. de Vries, C.L. Cobb, R.M. Martin, J. Chem. Phys. 87 (1987) 5830.
[6] K. Kanda, H. Ito, K. Someda, K. Suzuki, T. Kondow, K. Kuchitsu, J. Phys. Chem. 93 (1989) 6020.
[7] K. Kanda, K. Suzuki, T. Kondow, H. Ito, K. Kuchitsu, Bull. Chem. Soc. Jpn. 67 (1994) 93.
[8] K. Kanda, H. Ito, K. Suzuki, T. Kondow, K. Kuchitsu, Chem. Phys. Lett. 185 (1991) 225.
[9] Y. Fukuda, Ph.D. Thesis, The University of Tokyo, Japan, 1983.
[10] R.F. Lake, H. Thompson, Proc. Roy. Soc. A 317 (1970) 187.
[11] D.S.C. Yee, C.E. Brion, J. Electron Spectrosc. Relat. Phenom. 8 (1976) 313.
[12] K. Ohno, H. Mutoh, Y. Harada, J. Am. Chem. Soc. 105 (1983) 4555.
[13] K. Ohno, Y. Harada, in: Z.B. Maksič (Ed.), Theoretical Models of Chemical Bonding, Part 3, Springer, Berlin, 1991, p. 199.
[14] E. Illenberger, A. Niehaus, Z. Phys. B 20 (1975) 33.
[15] A. Niehaus, Adv. Chem. Phys. 45 (1981) 399.
[16] K. Ohno, T. Takami, K. Mitsuke, T. Ishida, J. Chem. Phys. 94 (1991) 2675.
[17] T. Takami, K. Ohno, J. Chem. Phys. 96 (1992) 6523.
[18] T. Pasinszki, H. Yamakado, K. Ohno, J. Phys. Chem. 97 (1993) 12718.
[19] T. Pasinszki, H. Yamakado, K. Ohno, J. Phys. Chem. 99 (1995) 14678.
[20] N. Kishimoto, J. Aizawa, H. Yamakado, K. Ohno, J. Phys. Chem. A 101 (1997) 5038.
[21] Y. Yamakita, M. Yamauchi, K. Ohno, Chem. Phys. Lett. 322 (2000) 189.
[22] Y. Yamakita, R. Yokoi, K. Ohno, to be published.
[23] K.P. Huber, G. Herzberg, in: Molecular Spectra and Molecular Structure, vol. 4. Constants of Diatomic Molecules, Van Nostrand, Princeton, 1979.
[24] R.A. Sanders, A.N. Schweid, M. Weiss, E.E. Muschlitz Jr., J. Chem. Phys. 65 (1976) 2700.
[25] D.W. Setzer (Ed.), Reactive Intermediates in the Gas Phase, Academic press, New York, 1979.
[26] J.M. Hollas, T.A. Sutherley, Mol. Phys. 22 (1971) 213.
[27] E. Heilbronner, V. Hornung, K.A. Muszkat, Helv. Chim. Acta 53 (1970) 347.
[28] V. Čermák, J. Chem. Phys. 44 (1966) 3781.
[29] M.J. Frisch et al., GAUSSIAN 98 (Revision A.7), Gaussian, Inc, Pittsburgh PA, 1998.
[30] V. Čermák, A.J. Yencha, J. Electron Spectrosc. Relat. Phenom. 8 (1976) 109.
[31] K. Ohno, S. Matsumoto, K. Imai, Y. Harada, J. Phys. Chem. 81 (1984) 206.

[32] W. Allison, E.E. Muschlitz Jr., J. Electron Spectrosc. Relat. Phenom. 23 (1981) 339.
[33] K. Kanda, S. Katsumata, T. Nagata, Y. Ozaki, T. Kondow, K. Kuchitsu, A. Hiraya, K. Shobatake, Chem. Phys. 175 (1993) 399.
[34] K. Kanda, M. Kono, K. Shobatake, N. Ibuki, to be published.
[35] V. Čermák, J. Electron Spectrosc. Relat. Phenom. 6 (1975) 135.